Journal of Inorganic and Organometallic Polymers and Materials (2021) 31:923–933
https://doi.org/10.1007/s10904-020-01828-8

Correlating the Photophysical Properties with the *Cure Index* of Epoxy Nanocomposite Coatings

Ali Ashtiani Abdi[1] · Maryam Jouyandeh[2] · Henri Vahabi[2] · Meisam Shabanian[3] · Dominique Lafon-Pham[4] · Xavier Gabrion[5] · Pascal Laheurte[6] · Alireza Mahmoudi Nahavandi[7] · Mohammad Reza Saeb[2]

Received: 25 January 2020 / Accepted: 23 November 2020 / Published online: 5 January 2021

Abstract

Transparency is a crucial factor in developing functional and decorative thin films and coatings, but incorporation of nanoparticles into organic resins for improving their properties quite often makes them opaque. In this work, photophysical properties of epoxy/layered double hydroxide (LDH) nanocomposite coatings were correlated with the dispersion state of LDH in the epoxy resin. The quality of solid epoxy network was assessed in terms of the *Cure Index* (*CI*) in relation to the transparency of the films containing 0.1, 0.5, 0.7, 1.0, and 3.0 wt% Mg–Al–LDH and Zn–Al–LDHs. At high loadings, direct transmittance (Y_{Direct}) decreased, while the light scattering in the coatings improved with respect to the neat epoxy. The highest Zn–Al–LDH loading (3.0 wt%) slightly deteriorated the transparency (Y_{Direct} = 93.3), but it was still higher than that of epoxy nanocomposite containing 0.5 wt% Mg–Al–LDH (Y_{Direct} = 89.8). A *Good* label was assigned to the epoxy nanocomposites containing up to 1.0 wt% Zn–Al–LDH, while epoxy/Mg–Al–LDH nanocomposites were *Poor* in terms of the *CI* labeling when Mg–Al–LDH content was more than 0.1 wt%. An increase of about 28 °C in the T_g value after the addition of 0.1 wt% Zn–Al–LDH indicated that Zn–Al–LDH can make strong the interaction between the epoxy matrix and nanoplatelets. However, decrease in the T_g of the epoxy/Mg–Al–LDH nanocomposites was a signature of the weak interactions between the Mg–Al–LDH nanoplatelets and epoxy matrix due to inappropriate dispersion. In general, it was revealed for the first time that the *CI* enables correlating the chemical crosslinking with the photophysical properties of the epoxy/LDH nanocomposites.

Keywords Transparency · Epoxy coatings · Spectroradiometer · *Cure Index* · Layered double hydroxide

1 Introduction

Thermosetting polymers filled with nanoscale particles have experienced unprecedented growth over the past years [1–5]. Attempts devoted to this family of engineered materials were directed to exploit the polymer properties

Ali Ashtiani Abdi and Maryam Jouyandeh have contributed equally to this work.

Supplementary Information The online version of this article (https://doi.org/10.1007/s10904-020-01828-8) contains supplementary material, which is available to authorized users.

✉ Alireza Mahmoudi Nahavandi
amahmoodi@icrc.ac.ir

✉ Mohammad Reza Saeb
mrsaeb2008@gmail.com

[1] Department of Organic Colorants, Institute for Color Science and Technology, Tehran, Iran

[2] Université de Lorraine, CentraleSupélec, LMOPS, F-57000 Metz, France

[3] Faculty of Chemistry and Petrochemical Engineering, Standard Research Institute (SRI), P.O. Box 31745-139, Karaj, Iran

[4] Centre des matériaux des Mines d'Alès (C2MA), IMT Mines Alès, 30319 Alès cedex, France

[5] Department of Applied Mechanics, FEMTO-ST Institute, UFC/CNRS/ENSMM/UTBM, Univ. Bourgogne Franche-Comté, 25000 Besançon, France

[6] Laboratoire LEM3 UMR 7239, Universite de Lorraine, 57045 Metz, France

[7] Color Imaging and Color Image Processing Department, Institute for Color Science and Technology, Tehran, Iran

like flexibility, easy casting and processability, and light weight, which were dramatically enhanced or sometimes granted extra properties by introducing nanoparticles [6–11]. However, success depends on the uniformity of dispersion as well as the loading content of the filler [12–15]. Typically, incompatibility between filler particles and the polymeric matrix causes a thermodynamic-driven particle agglomeration and phase separation. This kind of biphasic mixture, not only has no benefits but also sometimes results in a total loss in the properties of the neat polymeric vehicle [16–18].

Evaluating the quality of dispersion is possible either by different conventional instrumental techniques such as optical microscopy, scanning electron microscopy, transmission electron microscopy, and rheological techniques or emerging combinatorial techniques [19–21]. However, the quality of dispersion has another physical demonstration that is sometimes easily recognizable by eyes, i.e., transparency. Well-dispersed nanoscale size fillers in the matrix will not alter the direction of passing light. In this case, the only possible phenomena involved with fillers can be any probable light absorption. As the agglomerates grow, larger particles will change the path of the incident beam and cause light scattering. Therefore, an easy way to recognize the dispersion state of nanoparticles within a polymeric matrix is the evaluation of the polymeric nanocomposite's transparency. Although nanocomposites and transparency have been the subject of many investigations [22–25], to the best of our knowledge, rarely if not ever, the focus has been on the correlation of transparency of epoxy nanocomposites specifically with the goodness of curing.

Transparency of thin films, other than an indication for the quality of dispersion has important characteristics to determine the applications as or in optical elements [26–28], optical lenses [27, 29], electronic papers [30, 31], solar cell substrates [32, 33], organic light-emitting diodes, OLEDs [34, 35], and electrical insulating materials [36].

In this work, a spectroradiometer apparatus was applied for evaluating the light transmittance of epoxy-containing two kinds of platy layered double hydroxide (LDH), i.e., divalent Mg–Al–LDH and Zn–Al–LDH, intercalated with NO_3 interlayer ions and sodium dodecylbenzene sulfonate (SDBS) to study the dispersibility of 2D nanoparticles in an epoxy matrix. The state of transparency of the thin films was crosschecked by the curing state of the prepared nanocomposites by means of the *Cure Index* (*CI*) [37, 38]. The difference between the curing potential of samples filled with Mg–Al–LDH and Zn–Al–LDH was established in terms of *Poor*, *Good*, and *Excellent* labels assigned to the prepared thin coatings. The correlation between photophysical properties and chemical crosslinking was examined in epoxy nanocomposites containing 0.1, 0.3, 0.5, 0.7, 1.0, and 3.0 wt% platy nanoparticles.

2 Materials and Methods

2.1 Materials

Magnesium nitrate, zinc nitrate, aluminum nitrate, sodium hydroxide, sodium dodecylbenzene sulfonate (SDBS) were provided from Merck Co. (USA) for the synthesis of Mg–Al–SDBS–LDH and Zn–Al–SDBS–LDH. Bisphenol A/epichlorohydrin derived epoxy resin under the trade name of EPON™ 828 with density of 1.16 g/cm^3, viscosity of 110–150 P and epoxide equivalent weight (EEW) of 185–192 g/Equiv. was purchased from Huntsman Co., USA. Cycloaliphatic amine-based curing agent (EPIKURE F205) was provided from Hexion, Inc. (Columbus, USA). Cardura™ E10P glycidyl ester with density of 0.97 g/cm^3, viscosity of 7.13 mPa s and epoxy equivalent weight of 235–244 g/mol was used as a reactive diluent for epoxy resin provided from Hexion, Inc. (USA).

2.2 Preparation of Epoxy Nanocomposites

Transparent epoxy-based nanocomposite coatings were prepared by the addition of Mg–Al–SDBS–LDH and Mg–Al–SDBS–LDH into epoxy resin matrix [39]. More details on the preparation of LDH-based nanocomposites are available in our previous works [40, 41]. In order to investigate the influence of nanofiller loading on the curing reaction of epoxy resin and the transparency of the epoxy film, five different samples were prepared with different filler-to-resin weight ratios of 0.1, 0.5, 0.7, 1 and 3 wt%. Nanoparticles were dispersed into the mixture of epoxy resin and reactive diluent (10 wt%) by sonication for 15 min. Finally, the stoichiometric amount of F205 curing agent with (resin + reactive diluent):(hardener) weight ratio of 100:50 was thoroughly mixed with epoxy nanocomposites. Then, the samples were applied on steel substrates with 200 µm film applicator and had been left for ambient curing for 7 days. Then, the films were post-cured at 130 °C to ensure complete curing. This procedure guarantees the thorough curing reaction specifically for highly loaded samples in which the chain movements are restricted [42]. Finally, free films were delaminated from the substrate by immersing samples in distilled water for a couple of nights and drying in a vacuum oven at 70 °C for 1 h.

2.3 Characterization

2.3.1 Fourier Transform Infrared Spectroscopy (FTIR)

The FTIR synthesized LDH nanoplatelets were characterized by using a Fourier transform infrared spectrometer (FTIR, Perkin Elmer Spectrum Version 10.03.06). The dried powders were ground with KBr powder followed by FTIR spectroscopy in the frequency range of 4000 to 400 cm^{-1}. ATR characterization of the fully cured neat epoxy and the epoxy nanocomposite films containing 0.1 wt% of Mg–Al–LDH and Zn–Al–LDH was performed using Perkin Elmer Spectrum one apparatus.

2.3.2 X-Ray Diffraction Analysis (XRD)

XRD patterns were recorded by a Philips X'pert Pro MPD with a Cu K_α (k = 0.154 nm) radiation in a 2θ range of 10°–90° at 0.021 step size and 0.9 s per point measuring time. For characterization of the fully cured neat epoxy and the epoxy nanocomposite films containing 0.1 wt% of Mg–Al–LDH and Zn–Al–LDH an Xpert PANalytical Empyrean Serie II Alpha 1 (λ = 1.54442 Å) was used operating at 40 mA with a step of 0.05° in the 2θ angle range of 2°–100°.

2.3.3 Thermogravimetric Analysis (TGA)

TGA thermograms of neat epoxy, EP/Mg–Al–LDH and EP/Zn–Al–LDH were collected by a Perkin Elmer, Pyris Diamond in the temperature range of 25–650 °C by heating rate of 10 °C/min under nitrogen atmosphere.

2.3.4 Spectroradiometry

In order to investigate the photophysical characteristics of the LDH nanocomposites, inspired by the idea of solutions Turbidimetry/Nephelometry (ASTM D6855) and transmission haze (ASTM D1003), a spectroradiometer (Konica Minolta, CS 2000) was set up, as shown in Fig. 1. We arranged the measurements with Konica Minolta CS 2000 spectroradiometer, which is an ideal instrument for extremely low luminances. In this way, very low light signals due to the scattering of the incident light by nanofiller can be detected. Our experimental homemade set up is a close resemblance of conventional d/8° spectrophotometers with transmission haze mode [43, 44].

Standard white ceramic tile was initially illuminated by 12 V switching direct powered collimated beam of an incandescent light source (50 W, 2700 K), and the corresponding spectral radiance (L1) was recorded while the neat epoxy film without nanofiller (reference) was in the position of the sample. An aperture between the sample and the light source

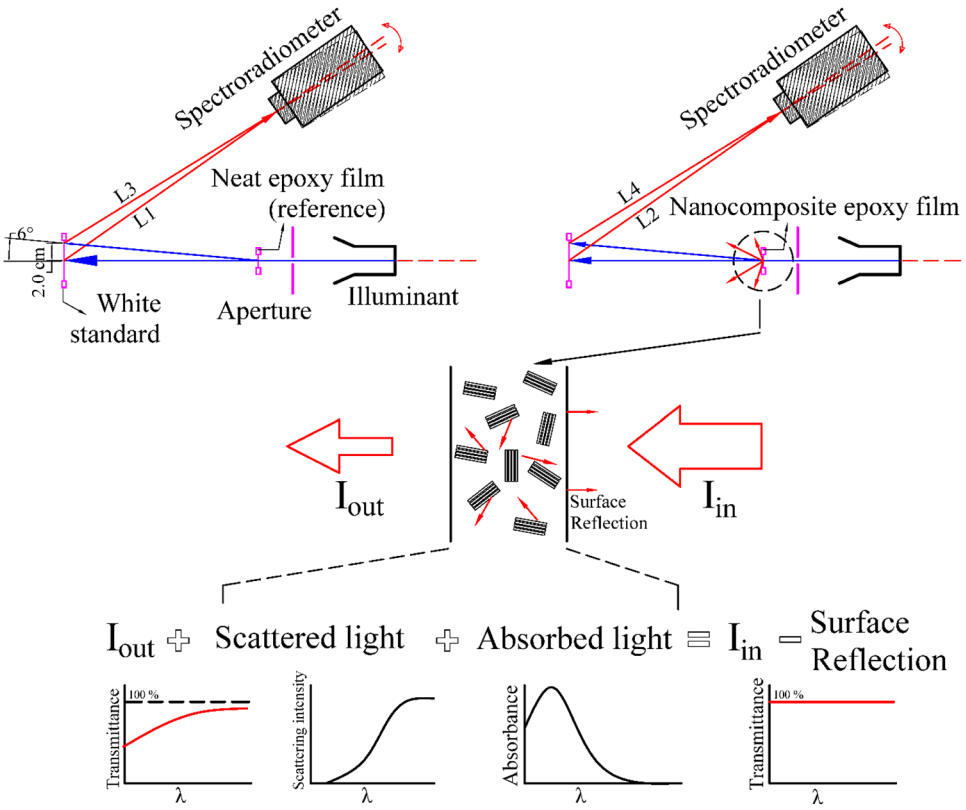

Fig. 1 Schematic setup for measuring light transmittance with direct and tilted (0°/6°) geometries

will ensure the elimination of the unwanted rays. The LDH epoxy samples were then located in the position to record the light radiance at the tile center (L2). At least three different points on each sample film were tested, and the average was finally reported.

After this step, a new adjustment was made by pointing the spectroradiometer to a position 2 cm far from the center of the white standard reference tile. Considering the distance of the sample holder to the standard white ceramic, an angle of 6° was made in between incident light and measuring point (0°/6° tilted geometry). Finally, a set of radiance measurements for the neat epoxy film (L3) as well as samples (L4) were performed in this new geometry.

The interaction of light with the samples was modeled by considering both absorption and scattering phenomena. Neat film as a reference medium has an advantage in excluding the effect of surface reflection. This is similar to the technique of using cuvette containing pure solvent in the calibration step in transmission spectrometers in order to get rid of solvent absorption and discontinuity of the media.

It should be noted that the repeatability of the proposed method is highly sensitive to film defects, such as the presence of air gaps, scratches, stains, fingerprints, and deformations.

2.3.5 Differential Scanning Calorimetry

Non-isothermal curing reaction of the prepared epoxy nanocomposites was recorded by Perkin Elmer DSC 4000 instrument. The fresh nanocomposites of about 12 mg were placed in a disposable aluminum pan heated from 15 to 300 °C at a heating rate of 10 °C/min under nitrogen purging. Then, at a constant heating rate, the samples were cooled to ambient temperature and again heated up to 300 °C to evaluate the glass transition temperature of the nanocomposites.

3 Results and Discussions

3.1 Characterization of the Synthesized LDH and Prepared Nanocomposites

The FTIR spectra and XRD patterns of Mg–Al–SDBS–LDH and Zn–Al–SDBS–LDH samples are shown in Figs. S1 and S2, respectively.

Figure 2 shows the FTIR spectra of fully cured neat epoxy and its nanocomposites containing 0.1 wt% of Mg–Al–LDH and Zn–Al–LDH. The peaks at around 3300–3500 cm^{-1} were related to stretching vibration bonds of hydroxyl groups. Aromatic ring stretching vibration absorption has also appeared at around 800 cm^{-1} and 1500 cm^{-1}. Moreover, two absorptions at 1040 cm^{-1} and 1240 cm^{-1} confirm the presence of C–O–C and C–N stretching, respectively. The

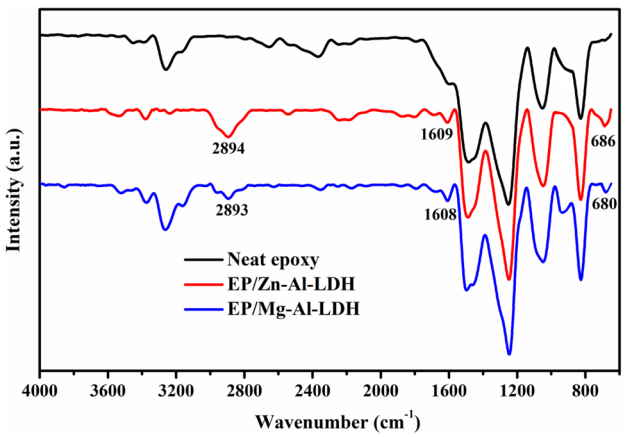

Fig. 2 FTIR spectra of neat epoxy, EP/Zn–Al–LDH and EP/Mg–Al–LDH

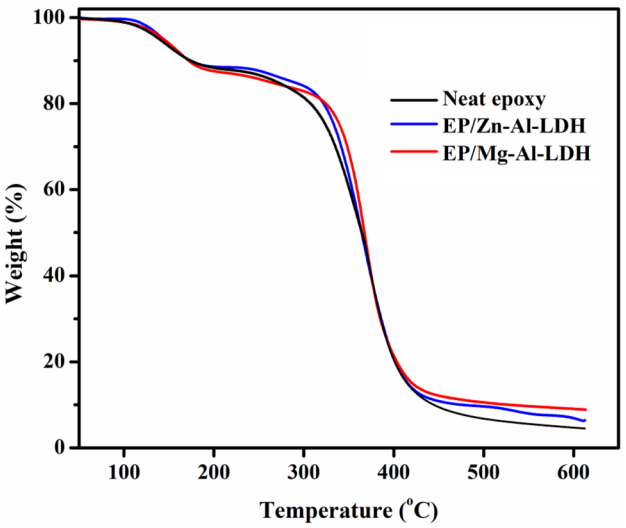

Fig. 3 TGA thermograms of neat epoxy, EP/Zn–Al–LDH and EP/Mg–Al–LDH

new appeared band at the FTIR spectra of EP/Zn–Al–LDH and EP/Mg–Al–LDH at about 1608 cm^{-1} belongs to the bending of interlayer water molecules of LDH. The peaks at low frequency region at about 680 cm^{-1} in the FTIR are assigned to the Zn–O in EP/Zn–Al–LDH and Mg–O in EP/Mg–Al–LDH as well as Al–O in the both of LDH incorporated epoxy nanocomposites [45–47]. The SDBS C–H stretching vibrations of LDH nanoplatelets can be observed at about 2930 and 2860 cm^{-1}.

The X-ray diffractograms of the fully cured neat epoxy and its nanocomposites containing 0.1 wt% of Mg–Al–LDH and Zn–Al–LDH are shown in Fig. S3.

Thermal degradation behavior of the cured neat epoxy and its nanocomposites containing 0.1 wt% of Mg–Al–LDH and Zn–Al–LDH under nitrogen atmosphere is presented in

Table 1 Thermal degradation parameters of neat epoxy and its nanocomposites

Sample	$T_{5\%}$ (°C)	$T_{20\%}$ (°C)	T_{max} (°C)	Residue (%)
Neat epoxy	139.4	307.2	366.3	4.8
EP/Zn–Al–LDH	143.2	322.0	368.1	6.9
EP/Mg–Al–LDH	144.0	324.3	369.2	9.1

Fig. 3. $T_{5\%}$, $T_{20\%}$ and T_{max}, which represent decomposition temperature of 5%, 20% and peak mass loss, respectively as well as char residue at temperatures of 600 °C are also reported in Table 1.

As can be seen in TGA thermograms a slight mass drop can observed in temperature below 200 °C which is related to evaporation of the small molecules such as solvent [48, 49]. The main weight loss of neat epoxy and its nanocomposites occurred in the temperate range of 300–450 °C due to polymer chain scissoring and decomposing of epoxy. The $T_{5\%}$, $T_{20\%}$ and T_{max} of the EP/Zn–Al–LDH and EP/Mg–Al–LDH were higher than that of neat epoxy which indicated that addition of LDH nanoplatelets to the epoxy matrix reduced the mobility of the epoxy chain around the nanoplatelets and enhanced thermal stability of network [50, 51]. EP/Zn–Al–LDH and EP/Mg–Al–LDH samples exhibited a higher value of the char residue compared to the neat epoxy because of presence of thermally stable LDH nanoplatelets in the epoxy system.

3.2 Photophysical Characteristics of Nanocomposites

The ratio of L2 to L1, which is known as transmittance (T1), shows the impact of nanofillers on the light signal, as shown in Fig. 4. The shadows are the standard error for at least three measurements from different locations on the sample. However, compared with neat epoxy, the transmittance remains above 90% in the range of 380–780 nm for low concentrations of Mg–Al–LDH (< 0.1%) and medium levels of Zn–Al–LDH (< 1%), confirming the excellent transparency.

According to Fresnel's law of surface reflection, when the light beam passes through the air/epoxy film interface in the neat epoxy film and then exits from the other side, about 4–6% of the light diminishes depending on the refraction index of the film. Note that the surface reflection from the neat epoxy film has been considered in the measurements, as illustrated in Fig. 1. Therefore, any drop in the transmittance spectrum is caused by the filler particles. By incorporating the nanoparticles into the epoxy film, the light might be absorbed and/or scattered by filler particles. Scattering of a photon mainly occurs when it meets filler particles of equal or bigger size with respect to its wavelength [52]. However, it has been reported in the literature that the Mg/Al and Zn/Al LDH has absorption mostly in shorter wavelengths than 350 nm [53–55]. Though, we may consider the absorption while studying the transmittance of these LDH nanocomposites. On the other hand, it is known that Zn–Al–LDH shows the luminescence in this composite [56] which makes it more complex to distinguish scattering and absorbance phenomena from direct transmittance measurements, in which the angle between the incident light and the point where the detector (spectroradiometer) reads the signal is zero. Therefore, the geometry is identical to the conventional UV–Vis spectrophotometers. Although the direct transmittance will provide information on the extent of drop in clarity in general, but the role of scattering (in comparison with the absorbance) which is a symptom of poor dispersion in reducing the incident light is not clear.

In order to evaluate the transparency of the samples, Y stimulus (W_y in Eq. 1) of CIE tristimulus values were calculated using the equal-energy spectrum of the CIE 1931 Standard (2°) Observer according to ASTM-E308 for both direct (Eq. 2) and tilted (Eq. 3) geometries.

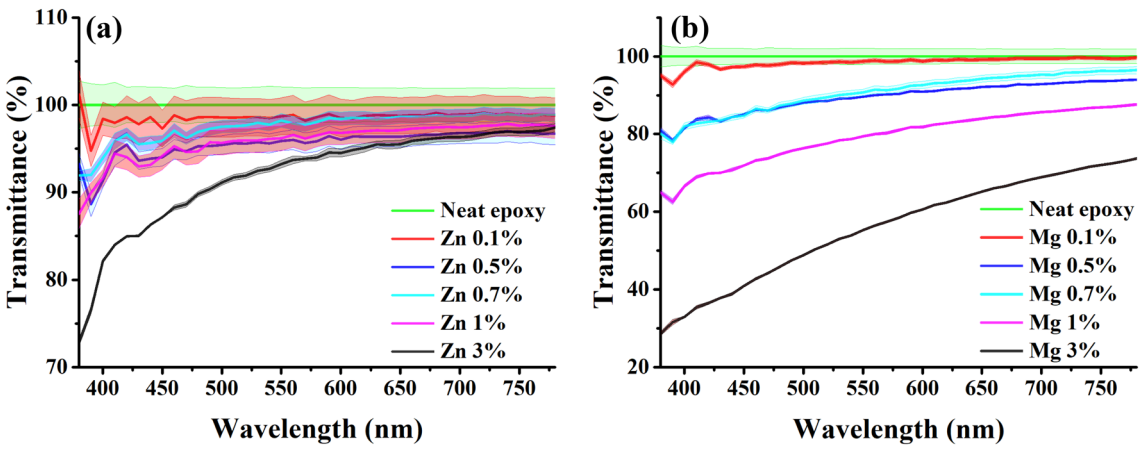

Fig. 4 Transmittance spectra of **a** EP/Zn–Al–LDH and **b** EP/Mg–Al–LDH samples. Shadows represent the standard error

$$Y_i = \int_{380}^{780} W_y(\lambda) T_i(\lambda) d\lambda, \quad (1)$$

$$T_{Direct} = (L2 - L1)/L1, \quad (2)$$

$$T_{tilted} = (L4 - L3)/L1. \quad (3)$$

As Y increases, the films become more transparent. Y corresponds to the light perception of human vision system, and slight changes can be detected in transparency of the samples with the help of high resolution instruments, as shown in Table 2. Trends in Y_{Direct} and Y_{tilted} in the absence of strong absorption will support each other. The direct transmittance, hence the Y_{Direct}, reduced by increasing the nanofiller content, while the scattered light (Y_{tilted}) increased compared to the neat epoxy film. However, these changes are not identical in Zn–Al–LDH and Mg–Al–LDH epoxy composites. While the Mg–Al–LDH dropping the Y_{Direct} dramatically, but even highest level of Zn–Al–LDH (3 wt%) has very low defect on transparency (Y_{Direct}= 93.3) although is higher than EP/Mg–Al–LDH nanocomposite in 0.5 wt%. The results suggest that the portion of particles with the higher refractive index has been increased in the composition. Nevertheless, knowing the fact that the refractive index of the composite matrix is not the same as the reference sample, it is not convincible that the perceived haziness directly results from agglomerated fillers or unwanted defects from imperfect curing process, e.g., unreacted monomers or the change in the crystallinity. In the following section, the curing will be correlated to the transparency using the *CI*.

3.3 Curing Analysis

It was found that the transparency of the epoxy/LDH nanocomposite films varies with the type and content of LDH nanoplatelets. The state of dispersibility of nanoparticles in the epoxy thermoset matrix primarily affects the crosslinked network formation, which consequently affects the ultimate properties of the nanocomposite. Therefore, the crosslinking reaction of the epoxy containing 0.1, 0.5, 0.7, 1, and 3 wt% of Mg–Al–LDH and Zn–Al–LDH nanoplatelets was investigated through non-isothermal DSC analysis. The DSC thermograms of curing reaction of epoxy composites containing various amounts of Mg–Al–LDH and Zn–Al–LDH nanoplatelets are shown in Fig. 5. As can be observed, an exothermic peak appeared for neat epoxy and its nanocomposites, which corresponds to the ring-opening reaction between the epoxide and the amine groups of the curing agent [57, 58]. The appearance of a small shoulder at higher temperatures is attributed to the ring-opening reaction between the epoxy and hydroxyl groups. The hydroxyl groups are formed during the reaction of epoxy groups with primary and secondary amines which have less reactivity, so participate in the epoxide ring via etherification reaction at the late stage of curing [59]. It is clear from Fig. 5 that the shape of DSC thermograms changed by increasing the nanoparticle content, particularly for the epoxy nanocomposites containing Zn–Al–LDH.

Here, for a deeper understanding of curing reaction of epoxy in the presence of LDH nanoplatelets, the values of the onset, peak and ending temperatures of the curing process (T_{onset}, T_p and T_{endset}), $\Delta T = T_{endset} - T_{onset}$ and the released heat during the complete curing reaction (ΔH^{∞}) were extracted from DSC thermograms [60], as listed in Table 3. Also, the values of ΔT^* ($\Delta T_{\text{nanocomposite}}/\Delta T_{\text{neat epoxy}}$), ΔH^* ($\Delta H_{\text{nanocomposite}}/\Delta H_{\text{neat epoxy}}$) and the *CI* ($\Delta T^* \times \Delta H^*$) were also calculated from the DSC data, as reported in Table 3 [61, 62].

As can be seen from Table 3, the values of ΔH^{∞} for epoxy nanocomposites containing 0.1 wt% Mg–Al–LDH and Zn–Al–LDH increased compared to neat epoxy. At very low concentrations of 0.1 wt%, the probability of nanoplatelets aggregation is almost zero [63], making no significant defect on the transparency (Zn–Al LDH, Y_{Direct} = 98.6 and Mg–Al–LDH, Y_{Direct} = 98.7), indicating that nanoplatelets are dispersed suitably in the epoxy matrix. Under these conditions, the maximum surface area of the nanoplatelets is

Table 2 Stimulus Y of neat epoxy films and its nanocomposites containing Zn–Al–LDH and Mg–Al–LDH

Geometry	Y_{Direct}		Y_{tilted}		Ratio (Y_{tilted} / Y_{Direct})	
Filler content	EP/Zn–Al–LDH	EP/Mg–Al–LDH	EP/Zn–Al–LDH	EP/Mg–Al–LDH	EP/Zn–Al–LDH	EP/Mg–Al–LDH
Neat epoxy	100 (Ref.)		0 (ref.)		0	
0.1%	98.6	98.7	1.4	4.7	0.014	0.047
0.5%	95.8	89.8	1.8	6.0	0.018	0.067
0.7%	98.0	91.0	2.4	5.8	0.024	0.064
1.0%	96.3	79.7	2.0	10.5	0.020	0.131
3.0%	93.3	56.0	5.8	27.1	0.062	0.484

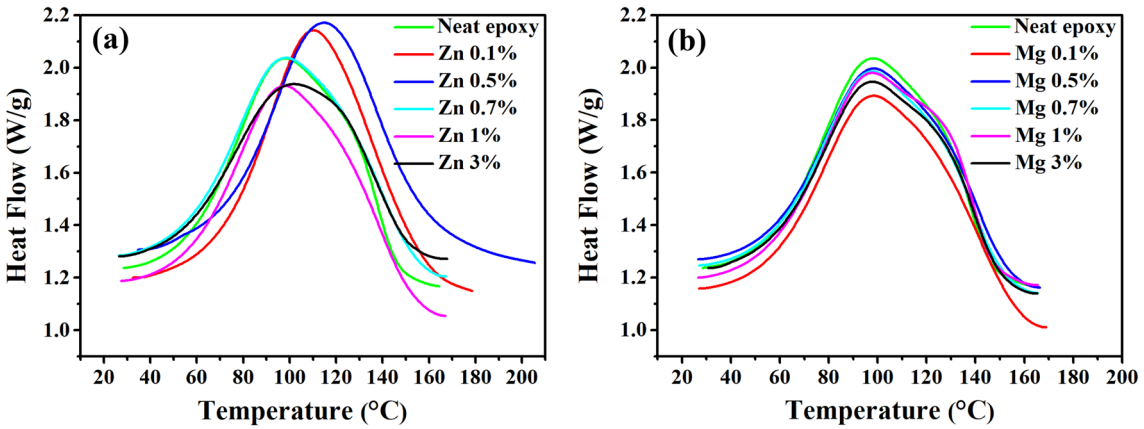

Fig. 5 Non-isothermal DSC thermograms of epoxy nanocomposites containing various contents of **a** Zn–Al–LDH and **b** Mg–Al–LDH at heating rate of 10 °C/min

Table 3 Curing characteristics of the prepared epoxy nanocomposites as a function of heating rate. The bold values and terms represent the quality of cure, as Poor, Good, or Excellent states

Sample	T_{Onset} (°C)	T_P (°C)	T_{Endset} (°C)	ΔT (°C)	ΔH_∞ (J/g)	$\Delta T°$	$\Delta H°$	CI	*Quality*
EP	28.4	97.9	164.5	136.1	303.2	n.a.	n.a.	n.a.	n.a.
Zn–Al–LDH									
0.1%	32.4	110.3	178.6	146.2	327.9	1.07	1.08	**1.16**	***Good***
0.5%	34.6	114.8	205.6	171.0	324.0	1.26	1.07	**1.34**	***Good***
0.7%	26.3	98.6	167.2	140.9	304.2	1.04	1.00	**1.04**	***Good***
1.0%	27.4	97.8	167.1	139.7	302.9	1.03	0.99	**1.02**	***Poor***
3.0%	26.4	99.1	167.8	141.4	256.7	1.04	0.85	**0.88**	***Poor***
Mg–Al–LDH									
0.1%	26.8	98.3	169.0	142.2	315.8	1.04	1.04	**1.08**	***Good***
0.5%	26.6	98.2	166.5	139.9	296.2	1.03	0.98	**1.01**	***Poor***
0.7%	26.9	97.6	165.5	138.5	296.7	1.02	0.98	**0.99**	***Poor***
1.0%	26.4	97.7	165.6	139.2	300.2	1.02	0.99	**1.01**	***Poor***
3.0%	30.7	97.8	165.4	134.7	286.2	0.99	0.94	**0.93**	***Poor***

n.a. Not applicable (reference measurements)

available for the resin to react with the functional groups of nanoplatelets, promoting the curing reaction. Nevertheless, by increasing the nanoplatelets concentration from 0.1 up to 3 wt%, the tendency of nanoplatelets to agglomerate increases, which is reflected by an increase in Y_{Direct} value. It is shown that nanoplatelets aggregation in the epoxy matrix hindered curing reaction, which results in lower ΔH^∞ values [64, 65]. The same results were obtained for the transparency of nanocomposite films due to the aggregation of Mg–Al–LDH nanoplatelets. However, for the case of epoxy nanocomposites containing well-dispersed Zn–Al–LDH, a slower decreasing trend is seen in the ΔH^∞ values by increasing the filler concentration. The relationship between the effect of nanoparticle dispersion in the formation of the epoxy network and the transparency of the epoxy coating is schematically shown in Fig. 6. Well-dispersion of nanoplatelets through the epoxy matrix results in the light beam pass through air/epoxy film border and exiting from the other side. However, the presence of agglomerated nanoplatelets in the resin matrix attenuates the light depending on the refractive index of the resulting matrix.

The curing state of the epoxy nanocomposites containing various amounts of Zn–Al–LDH and Mg–Al–LDH was determined based on CI by plotting ΔH^* versus ΔT^* (Fig. 7). Three zones are specified in Fig. 7; the green zone ($\Delta T^* < CI < \Delta H^*$) showing *Excellent* curing state, the blue zone is representing *Good* curing state ($CI > \Delta H^*$), and the red zone is indicating *Poor* curing state ($CI < \Delta T^*$) [37, 66]. In good agreement with their film transparency (Y_{Direct}), Epoxy nanocomposites containing 0.1, 0.5, and 0.7 wt% Zn–Al LDH have dispersed well according to the definition of *Good* label. This result means that Zn–Al–LDH nanoplatelets can effectively participate in the epoxide ring-opening and improve the crosslinking

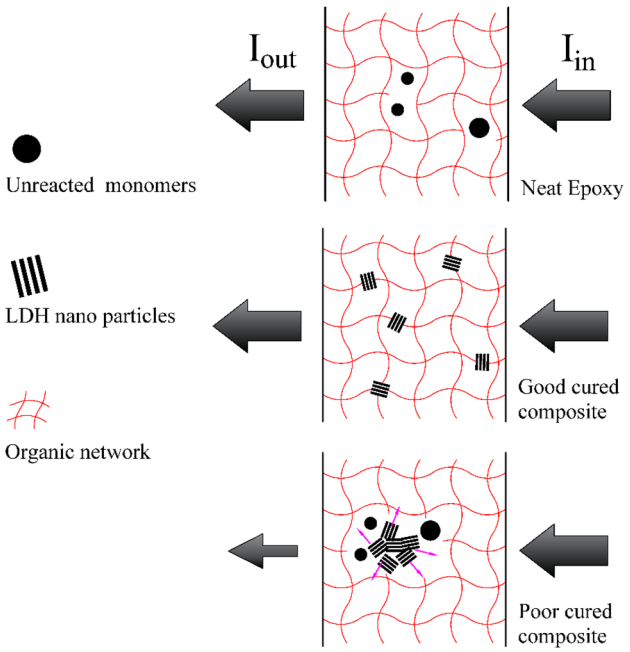

Fig. 6 Schematic diagram of the relationship between the nanoparticle dispersion in the epoxy and the transparency of the epoxy coating

density of the system. However, nanocomposites containing higher loadings of 1 and 3 wt% were labeled *Poor*. On the other hand, only epoxy nanocomposite containing 0.1 wt% Mg–Al–LDH was labeled *Good*. Mg–Al–LDH significantly decreased the Y_{Direct} value of the epoxy nanocomposite which indicates that some of the particles are larger than 380 nm and hinder the curing reaction, leading to *Poor* curing state.

3.4 Analysis of Glass Transition Temperature Variation

Table 4 shows the glass transition temperature (T_g) at a heating rate of 10 °C/min for fully cured neat epoxy and its nanocomposites containing 0.1, 0.5, 0.7, 1.0, and 3.0 wt% of Zn–Al–LDH and Mg–Al–LDH. There is an increase in T_g value after the addition of 0.1 and 0.5 wt% Zn–Al–LDH, indicating that Zn–Al–LDH can make strong interactions with the epoxy matrix, as was shown by *Good CI*. However, the T_g decreased by further increasing the Zn–Al–LDH content up to 3.0 wt%. By contrast, the T_g value of the epoxy/Mg–Al–LDH in all loadings was less than that of the neat epoxy. The variation of T_g reflects the ease of polymer chain's mobility and can be considered as evidence for the interactions between the nanoparticles and the epoxy matrix [67, 68]. The decrement of T_g in the epoxy/Mg–Al–LDH nanocomposites indicates the weak interactions between Mg–Al–LDH nanoplatelets and epoxy matrix due to inappropriate dispersion.

4 Conclusion

In this paper, photophysical aspects of transparency of epoxy nanocomposites containing 0.1, 0.5, 0.7, 1 and 3.0 wt% of Zn–Al–LDH and Mg–Al–LDH were investigated. It was shown that the transparency of such nanocomposites could be correlated to the light scattering, and the transparency makes sense of both dispersion quality and particle size of the fillers. Moreover, the dependency of dispersibility of nanoparticles in the epoxy matrix on its curing reaction

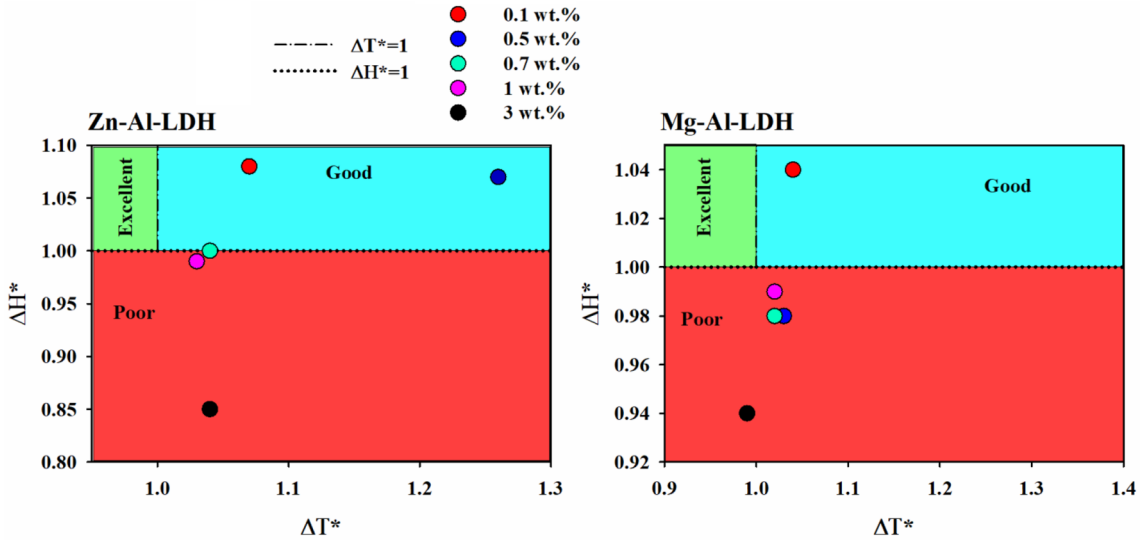

Fig. 7 Curing state of the epoxy nanocomposites containing 0.1, 05, 0.7, 1 and 3 wt% of Zn–Al–LDH and Mg–Al–LDH at a heating rate of 10 °C/min

Table 4 The glass transition temperature of fully cured neat epoxy and its nanocomposites containing Zn–Al–LDH and Mg–Al–LDH at a heating rate of 10 °C/min

Sample		T_g (°C)
Neat epoxy		67.94
Filler content	EP/Zn–Al–LDH	EP/Mg–Al–LDH
0.1%	96.39	65.58
0.5%	97.31	65.55
0.7%	62.94	64.69
1.0%	62.84	66.21
3.0%	67.80	65.34

was confirmed by introducing the *Cure Index*. Spectroradiometery indicated that the increasing of LDH nanoplatelets content decreased the Y_{Direct} value while increased the Y_{tilted} value, revealing the dependency of the dispersion state on the transparency of the nanocomposites. The transparency was also affected by the type of cation in the LDH. In the case of Mg–Al–LDH, the Y_{Direct} decreased significantly from 98.7 to 0.1 wt% to 56.0 for 3 wt%. By contrast, a slight decrease (from 96.8 to 93.3) was observed in the transparency of epoxy/Zn–Al LDH nanocomposites by increasing the concentration of nanoplatelets from 0.1 to 3 wt%. As a result, it can be inferred that Zn–Al LDH showed better dispersion in the epoxy matrix compared to the Mg–Al–LDH as proved by the *Good CI* for the former and the *Poor CI* for the latter. Moreover, a considerable increase in T_g values of epoxy/Zn–Al LDH nanocomposites at 0.1 (96.39 °C) and 0.5 wt% (97.31 °C) was observed compared to neat epoxy (67.94 °C) which indicates the appropriate dispersion of this nanoplatelets in the epoxy and their strong interaction with the matrix. Given that our findings are based on a limited type of nanofillers, the results from such a report should thus be treated as an initial idea to draw more attention to this technique.

The notion of the measurement of scattered light could be done using conventional DSLR cameras. Due to the fact that these devices are somehow colorimetric, a linear regression over RGB channels data can acceptably predict the Y stimulus. This could be more valuable when the camera can monitor the whole transmission pattern as a single image which is more informative than a single spot measurement done in the current study. This is the subject of our future studies.

Acknowledgements Special thanks goes to Dr. Mahzyar Gorji for his perceptive comments on the idea of evaluating the dispersion in terms of light scattering.

References

1. J. Jordan et al., Experimental trends in polymer nanocomposites—a review. Mater. Sci. Eng. A **393**(1–2), 1–11 (2005)
2. Y.-W. Mai, Z.-Z. Yu, *Polymer Nanocomposites* (Woodhead Publishing, Sawston, 2006).
3. M. Jouyandeh et al., Highly curable self-healing vitrimer-like cellulose-modified halloysite nanotube/epoxy nanocomposite coatings. Chem. Eng. J. **396**, 125196 (2020)
4. F. Seidi et al., Metal-organic framework (MOF)/epoxy coatings: a review. Materials **13**(12), 2881 (2020)
5. F. Seidi et al., Polyhedral oligomeric silsesquioxane/epoxy coatings: a review. Surf. Innov. (2020). https://doi.org/10.1680/jsuin.20.00037
6. M. Jouyandeh et al., Cure kinetics of epoxy/graphene oxide (GO) nanocomposites: effect of starch functionalization of GO nanosheets. Prog. Org. Coat. **136**, 105217 (2019)
7. M. Jouyandeh et al., High-performance epoxy-based adhesives reinforced with alumina and silica for carbon fiber composite/steel bonded joints. J. Reinf. Plast. Compos. **35**(23), 1685–1695 (2016)
8. M. Aliakbari et al., Multi-nationality epoxy adhesives on trial for future nanocomposite developments. Prog. Org. Coat. **133**, 376–386 (2019)
9. A. Rezvani Moghaddam et al., Tuning the network structure of graphene/epoxy nanocomposites by controlling edge/basal localization of functional groups. Ind. Eng. Chem. Res. **58**(47), 21431–21440 (2019)
10. A. Pratap et al., Dielectric behavior of nano barium titanate filled polymeric composites. Int. J. Mod. Phys. Conf. Ser. **22**, 1–10 (2013)
11. S.K. Kandasamy, K. Kandasamy, Recent advances in electrochemical performances of graphene composite (graphene–polyaniline/polypyrrole/activated carbon/carbon nanotube) electrode materials for supercapacitor: a review. J. Inorg. Organomet. Polym. Mater. **28**(3), 559–584 (2018)
12. M. Rong, M. Zhang, W. Ruan, Surface modification of nanoscale fillers for improving properties of polymer nanocomposites: a review. Mater. Sci. Technol. **22**(7), 787–796 (2006)
13. W. Gacitua, A. Ballerini, J. Zhang, Polymer nanocomposites: synthetic and natural fillers a review. Maderas. Cienc. tecnol. **7**(3), 159–178 (2005)
14. F. Tikhani et al., Cure Index demonstrates curing of epoxy composites containing silica nanoparticles of variable morphology and porosity. Prog. Org. Coat. **135**, 176–184 (2019)
15. M. Jouyandeh et al., Curing epoxy with polyethylene glycol (PEG) surface-functionalized $Ni_xFe_{3-x}O_4$ magnetic nanoparticles. Prog. Org. Coat. **136**, 105250 (2019)
16. H. Vahabi et al., Short-lasting fire in partially and completely cured epoxy coatings containing expandable graphite and halloysite nanotube additives. Prog. Org. Coat. **123**, 160–167 (2018)
17. M. Jouyandeh et al., Nonisothermal cure kinetics of epoxy/$Zn_xFe_{3-x}O_4$ nanocomposites. Prog. Org. Coat. **136**, 105290 (2019)
18. M. Jouyandeh et al., Curing epoxy with electrochemically synthesized $Zn_xFe_{3-x}O_4$ magnetic nanoparticles. Prog. Org. Coat. **136**, 105246 (2019)
19. S. Morsch et al., Molecularly controlled epoxy network nanostructures. Polymer **108**, 146–153 (2017)
20. S. Morsch et al., Insights into epoxy network nanostructural heterogeneity using AFM-IR. ACS Appl. Mater. Interfaces **8**(1), 959–966 (2016)
21. M. Jouyandeh et al., Curing epoxy with polyvinylpyrrolidone (PVP) surface-functionalized $Ni_xFe_{3-x}O_4$ magnetic nanoparticles. Prog. Org. Coat. **136**, 105259 (2019)

22. S. Srivastava, M. Haridas, J. Basu, Optical properties of polymer nanocomposites. Bull. Mater. Sci. **31**(3), 213–217 (2008)
23. C. Sanchez et al., Optical properties of functional hybrid organic–inorganic nanocomposites. Adv. Mater. **15**(23), 1969–1994 (2003)
24. W. Caseri, Nanocomposites of polymers and metals or semiconductors: historical background and optical properties. Macromol. Rapid Commun. **21**(11), 705–722 (2000)
25. Y. Imai et al., Transparent poly (bisphenol A carbonate)-based nanocomposites with high refractive index nanoparticles. Eur. Polym. J. **45**(3), 630–638 (2009)
26. H. Althues, J. Henle, S. Kaskel, Functional inorganic nanofillers for transparent polymers. Chem. Soc. Rev. **36**(9), 1454–1465 (2007)
27. Y.-Q. Li et al., Facile synthesis of highly transparent polymer nanocomposites by introduction of core–shell structured nanoparticles. Chem. Mater. **20**(8), 2637–2643 (2008)
28. Z.K. Heiba, M.B. Mohamed, N. Imam, Photophysical parameters of functional transparent polymethyl-methacrylate/double-walled carbon nanotubes nanocomposite sheet under UV-irradiation. J. Inorg. Organomet. Polym. Mater. **26**(4), 780–787 (2016)
29. K.C. Krogman, T. Druffel, M.K. Sunkara, Anti-reflective optical coatings incorporating nanoparticles. Nanotechnology **16**(7), S338 (2005)
30. D.-W. Wang et al., Fabrication of graphene/polyaniline composite paper via in situ anodic electropolymerization for high-performance flexible electrode. ACS Nano **3**(7), 1745–1752 (2009)
31. Z. Weng et al., Graphene–cellulose paper flexible supercapacitors. Adv. Energy Mater. **1**(5), 917–922 (2011)
32. X.Y. Zeng et al., A new transparent conductor: silver nanowire film buried at the surface of a transparent polymer. Adv. Mater. **22**(40), 4484–4488 (2010)
33. Z. Yin et al., Organic photovoltaic devices using highly flexible reduced graphene oxide films as transparent electrodes. ACS Nano **4**(9), 5263–5268 (2010)
34. S. Ummartyotin et al., Development of transparent bacterial cellulose nanocomposite film as substrate for flexible organic light emitting diode (OLED) display. Ind. Crops Prod. **35**(1), 92–97 (2012)
35. J. Jin et al., Silica nanoparticle-embedded sol–gel organic/inorganic hybrid nanocomposite for transparent OLED encapsulation. Org. Electron. **13**(1), 53–57 (2012)
36. C. Park et al., *Electrically Conductive, Optically Transparent Polymer/Carbon Nanotube Composites and Process for Preparation Thereof*. 2009, National Aeronautics, Space Administration (NASA), U.S. Patent No. 7,588,699
37. M. Jouyandeh et al., 'Cure Index' for thermoset composites. Prog. Org. Coat. **127**, 429–434 (2019)
38. M. Jouyandeh et al., Curing epoxy with polyvinylpyrrolidone (PVP) surface-functionalized $Zn_xFe_{3-x}O_4$ magnetic nanoparticles. Prog. Org. Coat. **136**, 105227 (2019)
39. H. Rastin et al., Transparent nanocomposite coatings based on epoxy and layered double hydroxide: nonisothermal cure kinetics and viscoelastic behavior assessments. Prog. Org. Coat. **113**, 126–135 (2017)
40. M. Shabanian et al., Novel nanocomposites consisting of a semicrystalline polyamide and Mg–Al LDH: morphology, thermal properties and flame retardancy. Appl. Clay Sci. **90**, 101–108 (2014)
41. M. Hajibeygi, M. Shabanian, H.A. Khonakdar, Zn–Al LDH reinforced nanocomposites based on new polyamide containing imide group: from synthesis to properties. Appl. Clay Sci. **114**, 256–264 (2015)
42. Z. Karami et al., Epoxy/layered double hydroxide (LDH) nanocomposites: synthesis, characterization, and excellent cure feature of nitrate anion intercalated Zn–Al LDH. Prog. Org. Coat. **136**, 105218 (2019)
43. F.W. Billmeyer Jr., Y. Chen, On the measurement of haze. Color Res. Appl. **10**(4), 219–224 (1985)
44. R.S. Berns, *Billmeyer and Saltzman's Principles of Color Technology* (Wiley, New York, 2019).
45. L. Guo et al., A comparison of corrosion inhibition of magnesium aluminum and zinc aluminum vanadate intercalated layered double hydroxides on magnesium alloys. Front. Mater. Sci. **12**(2), 198–206 (2018)
46. Z. Karami et al., Curing epoxy with Mg–Al LDH nanoplatelets intercalated with carbonate ion. Prog. Org. Coat. **136**, 105278 (2019)
47. Z. Karami et al., Epoxy/Zn–Al–CO_3 LDH nanocomposites: curability assessment. Prog. Org. Coat. **138**, 105355 (2020)
48. S. Bayat et al., Thin films of epoxy adhesives containing recycled polymers and graphene oxide nanoflakes for metal/polymer composite interface. Prog. Org. Coat. **136**, 105201 (2019)
49. S.M.R. Paran et al., Thermal decomposition kinetics of dynamically vulcanized polyamide 6–acrylonitrile butadiene rubber–halloysite nanotube nanocomposites. J. Appl. Polym. Sci. **136**(20), 47483 (2019)
50. F. Seidi et al., Imidazole-functionalized nitrogen-rich Mg–Al–CO_3 layered double hydroxide for developing highly crosslinkable epoxy with high thermal and mechanical properties. Colloids Surf. A (2020). https://doi.org/10.1016/j.colsurfa.2020.125826
51. F. Seidi et al., Super-crosslinked ionic liquid-intercalated montmorillonite/epoxy nanocomposites: cure kinetics, viscoelastic behavior and thermal degradation mechanism. Polym. Eng. Sci. **60**(8), 1940–1957 (2020)
52. G. Mie, Contributions to the optics of turbid media, particularly of colloidal metal solutions (transl into English). Ann. Phys. (Leipz.) **25**(3, 1908), 377–445 (1976)
53. J.S. Valente et al., Adsorption and photocatalytic degradation of phenol and 2, 4 dichlorophenoxiacetic acid by Mg–Zn–Al layered double hydroxides. Appl. Catal. B **90**(3–4), 330–338 (2009)
54. S. Babakhani et al., Optical and thermal properties of Zn/Al-layered double hydroxide nanocomposite intercalated with sodium dodecyl sulfate. J. Spectrosc. (2014). https://doi.org/10.1155/2014/467064
55. X.-R. Wang et al., Fabrication of Zn–Ti layered double hydroxide by varying cationic ratio of Ti^{4+} and its application as UV absorbent. Chin. Chem. Lett. **28**(2), 394–399 (2017)
56. R. Tian, D. Yan, M. Wei, Layered double hydroxide materials: assembly and photofunctionality, in *Photofunctional Layered Materials*. 2015, Springer, Cham. p. 8
57. M. Jouyandeh et al., Curing epoxy with electrochemically synthesized $Gd_xFe_{3-x}O_4$ magnetic nanoparticles. Prog. Org. Coat. **136**, 105245 (2019)
58. M. Jouyandeh et al., Curing epoxy with electrochemically synthesized $Ni_xFe_{3-x}O_4$ magnetic nanoparticles. Prog. Org. Coat. **136**, 105198 (2019)
59. M. Jouyandeh et al., Curing epoxy with polyvinylpyrrolidone (PVP) surface-functionalized $Mn_xFe_{3-x}O_4$ magnetic nanoparticles. Prog. Org. Coat. **136**, 105247 (2019)
60. M. Jouyandeh et al., Protocol for nonisothermal cure analysis of thermoset composites. Prog. Org. Coat. **131**, 333–339 (2019)
61. F. Tikhani et al., Curing kinetics and thermal stability of epoxy composites containing newly obtained nano-scale aluminum hypophosphite ($AlPO_2$). Polymers **12**(3), 644 (2020)
62. M. Jouyandeh et al., Synthesis, characterization, and high potential of 3D metal–organic framework (MOF) nanoparticles for curing with epoxy. J. Alloys Compd **829**, 154547 (2020)
63. M. Jouyandeh et al., Surface engineering of nanoparticles with macromolecules for epoxy curing: development of super-reactive

nitrogen-rich nanosilica through surface chemistry manipulation. Appl. Surf. Sci. **447**, 152–164 (2018)
64. V. Akbari et al., Surface chemistry of halloysite nanotubes controls the curability of low filled epoxy nanocomposites. Prog. Org. Coat. **135**, 555–564 (2019)
65. Z. Karami et al., Cure Index for labeling curing potential of epoxy/LDH nanocomposites: a case study on nitrate anion intercalated Ni–Al–LDH. Prog. Org. Coat. **136**, 105228 (2019)
66. M. Jouyandeh et al., Bushy-surface hybrid nanoparticles for developing epoxy superadhesives. Appl. Surf. Sci. **479**, 1148–1160 (2019)
67. G. Psarras, Conductivity and dielectric characterization of polymer nanocomposites, in *Physical Properties and Applications of Polymer Nanocomposites*, 2010, Elsevier, Amsterdam, pp. 31–69
68. E. Koufakis et al., $ZnTiO_3$/epoxy resin nanocomposites: development, dielectric behaviour and functionality. Polym. Test. **77**, 105870 (2019)